Stoichiometric silver beta alumina studied at 25, 300 and 500 degrees C by powder neutron diffraction

1990 J. Phys.: Condens. Matter 2 2335

(http://iopscience.iop.org/0953-8984/2/10/001)

J. Phys.: Condens. Matter 2 (1990) 2335–2344. Printed in the UK

Stoichiometric silver beta alumina studied at 25, 300 and 500 °C by powder neutron diffraction

J M Newsam†‡, A K Cheetham† and B C Tofield§

† University of Oxford, Chemical Crystallography Laboratory, 9 Parks Road, Oxford OX1 3PD, UK

§ Materials Physics and Metallurgy Division, AERE Harwell, Chilton, Oxon OX11 0RA, UK

Received 20 December 1988, in final form 6 November 1989

Abstract. The structure of stoichiometric (S) silver beta alumina, $Ag_{1-x}Al_{11}O_{17+x/2}$; $x = 0.0$, prepared via hydrogen reduction of a non-stoichiometric (NS) material with $x = 0.45$ has been determined at 25 °C, 300 °C and 500 °C by Rietveld analyses of powder neutron diffraction data. In contrast to the single Ag site observed previously at 4.2 K, the silver ion distribution becomes increasingly diffuse with increasing temperature. At 25 °C the mirror plane structure is similar to that seen at 4.2 K, but apparently with some anti-Beevers–Ross site occupancy, and still with an increased c-axis constant compared with the NS parent. At 500 °C no silver cation site is well defined, consistent with a two-dimensional quasi-liquid state suggested by earlier diffuse x-ray scattering experiments.

1. Introduction

The non-stoichiometry of as-synthesised beta aluminas, $Na_{1+x}Al_{11}O_{17+x/2}$; $0.2 < x < 0.4$, and the structural and physical consequences of variations in the chemical composition, have been the focus of a considerable research effort involving many different groups (Kummer 1972, Bates and Farrington 1981; Newsam and Tofield 1981a, Kleitz *et al* 1983, Collongues *et al* 1984, Boyce *et al* 1985). Although generally troublesome to access synthetically, stoichiometric beta aluminas, $MAl_{11}O_{17}$, potentially provide a means of examining those structural and physical properties that derive from the beta alumina structure itself, as opposed to those that reflect the effects of chemical non-stoichiometry. We have earlier reported a convenient synthesis of stoichiometric silver beta alumina, $AgAl_{11}O_{17}$, from its non-stoichiometric counterpart, together with details of its structure at 4.2 K (Newsam and Tofield 1981b). At 4.2 K the structure is well ordered with a single, fully occupied silver site in each mirror plane section. Silver occupancy of this site, combined with a cooperative in-plane displacement of three adjacent O5 atoms, gives rise to an $a\sqrt{3} \times a\sqrt{3} \times c$ supercell (Boilot *et al* 1980, Newsam and Tofield 1981b) that, at this stoichiometric composition, develops long-range coherence. At temperatures close to ambient and above, however, x-ray scattering measurements (on approximately stoichiometric materials) imply that this long-range coherence is lost, the silver atom distribution becoming more diffuse and two-dimensional-liquid-like in character (Boilot *et al* 1980). We describe here the results of full structure analyses of stoichiometric silver beta alumina at 25 °C, 300 °C and 500 °C.

‡ Present address: Exxon Research and Engineering Company, Route 22 East, Annandale, NJ 08801, USA.

0953-8984/90/102335 + 10 $03.50

2. Experimental procedure

The sample of stoichiometric silver beta alumina, $AgAl_{11}O_{17}$, was derived from the highly non-stoichiometric material $Na_{1.45}Al_{11}O_{17.225}$ (England *et al* 1982) as described earlier (Newsam and Tofield 1981b). Briefly, this preparation route involved exchange in $AgNO_3$, D_2 reduction of the resulting non-stoichiometric silver beta alumina, and final heat treatment in a vanadium sample can. The non-stoichiometric to stoichiometric conversion occurs during the reduction step.

The $AgAl_{11}O_{17}$ sample was maintained in the 15 mm diameter, thin-walled vanadium can and powder neutron diffraction (PND) data were collected on the D1A diffractometer at the ILL, Grenoble (Hewat and Bailey 1976) at the temperatures 4.2 K (Newsam and Tofield 1981b), 298 K (25 °C), and 773 K (500 °C), and on the PANDA diffractometer at AERE Harwell at 573 K (300 °C). The data accumulation and collation procedures have been described previously (Newsam and Tofield 1981b, Newsam *et al* 1985) (the use of *odd, odd, odd* index reflections from Ge monochromators, (533) on D1A and (511) on PANDA, and, on D1A, the transmission properties of the neutron guide tubes (Hewat and Bailey 1976) gives rise to a negligible λ/n contamination in the PND patterns—see, e.g., figure 2 later)). The summed patterns contained contributions from 8, 3 and 6 counters for the 25 °C, 300 °C and 500 °C data, respectively. In the 500 °C D1A data, because of the instrumental geometry and the use of vanadium for the furnace element, the only significant peaks in the diffraction profile are those due to $AgAl_{11}O_{17}$ or silver metal (reflecting the stoichiometry excess in the starting material, $x = 0.45$; the silver is retained as a surface coating after the sample reduction and back-exchange steps). For the PANDA run at 300 °C, a tantalum element furnace was used, giving rise to three additional Ta_{metal} peaks. In refinement, those regions to which Ag_{metal} (or Ta_{metal}) reflections contributed significant intensity were excluded from the calculations. The low-angle regions were also omitted because of the asymmetrical deviations of the peak shapes from gaussian at low angles (see figure 2 below—satisfactory analytical descriptions of this peak asymmetry have since been described (Prince 1983, Howard 1982, van Laar and Yelon 1984)). The course of the Rietveld (1969) refinements (other than as discussed below), the refinement codes and the chosen scattering lengths were as described previously (Newsam and Tofield 1981b). In each case, space group $P6_3/mmc$ (No 194) was assumed and confirmed by the analyses. Experimental variables, final profile parameters and residuals are listed in table 1. Final atom positions and temperature factors are given in table 2.

For the 25 °C data, the refinements converged smoothly from the same starting model as used in analysis of the 4.2 K data set (Newsam and Tofield 1981b). The silver distribution in the mirror plane, however, was found to be significantly different. The predominant silver site is again of the 6h type (Wyckoff notation), with atomic coordinates of type $x\,2x\,\frac{1}{4}$ (Hahn 1983), with a value of $x \simeq -0.23$, close to the value $x = -0.224(1)$ observed at 4.2 K (Newsam and Tofield 1981b). The thermal components of the silver within the mirror plane are, however, increased considerably relative to those at 4.2 K. Further, even with this considerable thermal delocalisation, the population of the 6h site refined to significantly less than unity (the site populations are discussed as each being half of the product of the respective site occupancy and site multiplicity, and thus refer to the formula unit $AgAl_{11}O_{17}$, one half of the content of the unit cell). A series of models including other sites was therefore considered. It should be noted, however, that with neutron diffraction data the relative scattering power of silver is much smaller than in the x-ray case, preventing as detailed an analysis of silver site

Table 1. Experimental and optimised profile parameters with estimated standard deviations in parentheses.

	298 K (25 °C)	573 K (300 °C)	773 K (500 °C)
Instrument	D1A	PANDA	D1A
Apparatus	—	Ta-element furnace	V-element furnace
Wavelength (Å)	1.5118(1)	1.5279(5)†	1.5110(5)
a (Å)	5.5913(1)	5.6026(6)	5.6169(1)
c (Å)	22.5293(2)	22.5489(10)	22.5973(2)
Volume (Å^3)	609.96(2)	613.0(2)	617.42(4)
Zero point (deg)‡	−0.0804(7)	0.124(2)	−0.0303(8)
U (deg^2)§	0.090(1)	0.60(3)	0.105(2)
V (deg^2)	−0.227(3)	−0.54(4)	−0.260(5)
W (deg^2)	0.202(2)	0.19(1)	0.222(2)
R_B	0.042	0.052	0.039
R_p	0.083	0.091	0.080
R_{wp}	0.093	0.082	0.078
R_e	0.116	0.043	0.109

† Calculated from profile refinement of the silver metal contribution to the measured diffraction pattern.
‡ Counter zero-point error, $2\theta_{obs} - 2\theta_{calc}$.
§ Halfwidth parameters (U, V and W) and residuals as defined by Rietveld (1969).

distributions as have been considered for non- and near-stoichiometric samples using single-crystal x-ray data (Roth 1972, Colomban 1979, Boilot *et al* 1979a,b, 1980). The present preparation route to $AgAl_{11}O_{17}$ is suitable only for polycrystalline materials, the nature of which makes detailed quantitative analyses of powder x-ray diffraction data difficult. Schemes for a more extended static delocalisation about the above 6h site, involving a second silver atom at, or close to $-0.19\ 0.19\frac{1}{4}$ (6h) with independent temperature factors converged to reasonable residuals ($R_p = 0.0837$, $R_{wp} = 0.0933$) when the total occupancy was constrained to be unity. The individual occupancies were 0.51 and 0.49 respectively, but the U_{11} component of the former site was 0.25(2). Models involving the mid-oxygen (MO) and Beevers–Ross (BR) sites were also unsatisfactory in that the U_{11} components of silver on these sites adopted extremely large values (1.2(2) and 0.8(1) respectively). The anti-Beevers–Ross (ABR) site gave more acceptable convergences and it is this model that is presented in the tables. Even for this site, the U_{11} and U_{12} components are large, suggesting that some static disorder may also occur, although (perhaps reflecting the low occupancy and the diffuse nature of this position) sensible refinements involving slight displacements from the ABR site were not obtained.

When allowed to vary, the populations of the interstitial aluminium site, Al_i (Roth 1975, Reidinger 1979), and of Al1 converged to respective values of 0.02(4) and 5.91(5). These results are in good agreement with the analysis of the structure at 4.2 K (Newsam and Tofield 1981b), and confirm the absence of aluminium occupancy of the interstitial site in stoichiometric materials prepared via D_2 reduction of non-stoichiometric silver beta alumina. The final observed, calculated and difference profiles are displayed in figure 1. The low-angle region of the measured profile is plotted in figure 2, together with the reflection positions calculated on the basis of an $a\sqrt{3} \times a\sqrt{3} \times c$ supercell similar to that observed at 4.2 K (Boilot *et al* 1980, Newsam and Tofield 1981b).

Refinement of the 300 °C and 500 °C data sets parallelled that of the 25 °C data. The corresponding final overall and atomic parameters, and separations and angles are listed

Table 2. Final atomic parameters with estimated standard deviations in parentheses†.

Atom	Position	Site Symmetry	x	z	Population	U_{11}	U_{33}	U_{12}	U_{13}	U_{23}
O(1)	12k	m	0.1569(2)	0.0500(1)	6.0	0.0071(6)	0.0077(5)	0.0050(8)	−0.0017(6)	$-U_{13}$
			0.1557(6)	0.0495(2)		0.001(2)	−0.003(3)	0.002(2)	−0.004(2)	
			0.1577(2)	0.0501(1)		0.0134(6)	0.0145(8)	0.0103(8)	−0.0028(6)	
O(2)	12k	m	0.5021(3)	0.1459(1)	6.0	0.0074(8)	0.0113(8)	0.0044(8)	0.0011(6)	$-U_{13}$
			0.5025(6)	0.1467(2)		0.004(2)	0.003(3)	0.004(4)	0.002(1)	
			0.5026(3)	0.1460(1)		0.0097(6)	0.0194(8)	0.0023(10)	0.0028(6)	
O(3)	4f	3m	−0.3333	0.0551(1)	2.0	0.0052(10)	0.0077(13)	$U_{11}/2$	0	0
				0.0559(5)		−0.002(4)	0.034(8)			
				0.0553(2)		0.0133(11)	0.014(2)			
O(4)	4e	3m	0.0	0.1421(1)	2.0	0.0062(10)	0.0054(15)	$U_{11}/2$	0	0
				0.1416(6)		0.009(4)	0.043(10)			
				0.1422(2)		0.0114(11)	0.018(2)			
O(5)	6h	mm	0.306(2)	0.25	1.0	0.031(7)	0.007(3)	0.018(4)	0	0
			0.298(2)			−0.01(1)	0.008(8)	0.025(9)		
			0.311(5)			0.052(13)	0.006(3)	0.035(7)		
Al(1)	12k	m	−0.1665(4)	0.1067(1)	6.0	0.0032(7)	0.0121(10)	0.001(1)	0.0022(6)	$-U_{13}$
			−0.1657(13)	0.1066(3)		0.005(4)	0.013(3)	−0.006(6)	−0.006(3)	
			−0.1679(4)	0.1071(1)		0.0119(10)	0.015(1)	0.009(1)	0.0017(6)	
Al(2)	4f	3m	0.3333	0.0254(2)	2.0	0.0023(8)	0.007(2)	$U_{11}/2$	0	0
				0.0241(6)		0.027(5)	−0.005(8)			
				0.0253(2)		0.0071(11)	0.017(2)			
Al(3)	4f	3m	0.3333	0.1753(2)	2.0	0.009(1)	0.005(2)	$U_{11}/2$	0	0
				0.1791(5)		0.0011(5)	−0.02(8)			
				0.1752(2)		0.014(1)	0.010(3)			
Al(4)	2a	3m	0.0	0.0	1.0	0.009(2)	0.011(3)	$U_{11}/2$	0	0
						−0.016(6)	0.06(1)			
						0.007(2)	0.022(4)			
Ag(1)	6h	mm	−0.238(2)	0.25	0.74(5)‡	0.059(8)	0.011(8)	−0.038(7)	0	0
			−0.262(4)		0.66(9)	0.00(2)	0.08(3)	−0.02(1)		
			−0.246(6)		0.83(8)	0.32(7)	0.026(10)	−0.26(8)		
Ag(2)	2b	$\bar{6}$m2	0.0	0.25	0.26(5)‡	0.55(14)	0.02(3)	$U_{11}/2$	0	0
					0.34(9)	0.6(1)	−0.05(3)			
					0.17(8)	0.34(14)	0.01(4)			

† The parameters for each species are respectively those determined at 25 °C (D1A data—top row), 300 °C (PANDA—middle) and 500 °C (D1A—lower row). Difficulties in background estimation at high angles are reflected in some temperature factor matrices being non-positive-definite, noticeably for the PANDA data.

‡ Total Ag population constrained to equal 1.0 at each temperature—see text.

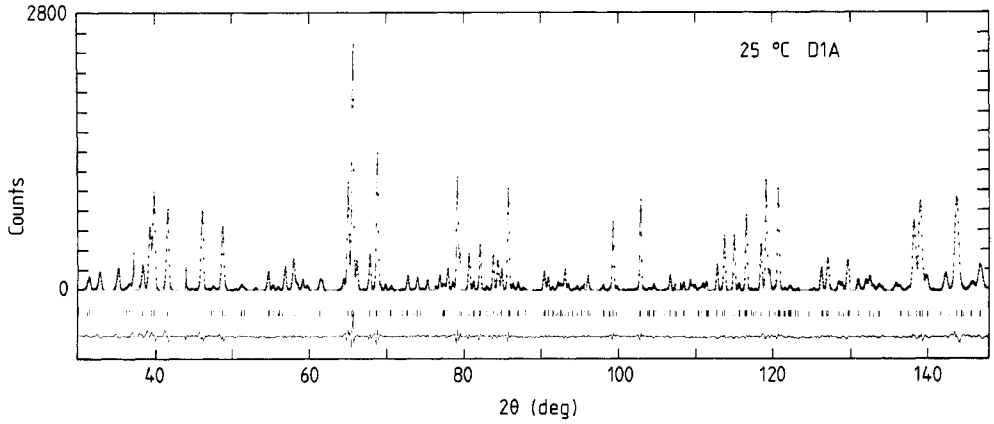

Figure 1. The final observed (dots), calculated (full curve connecting calculated points) and difference (lower trace) powder neutron diffraction profiles for stoichiometric silver beta alumina at 25 °C. The positions of the contributing reflections are marked by the faint vertical bars.

in tables 1–4. The final observed, calculated and difference profiles are shown in figures 3 and 4. At 300 °C, the structure definition is limited by the poorer quality and more limited range of the data set. In particular, the temperature factors are not as reliable as those determined using the D1A data. However, the atomic parameters broadly reflect the trend in structure evolution as the temperature is raised from 4.2 K to 500 °C.

3. Discussion and conclusion

The analysis of the 25 °C data manifests the onset of a transformation in the structure of $AgAl_{11}O_{17}$. The fully ordered mirror plane distribution which was apparent at 4.2 K (Newsam and Tofield 1981a) is no longer found and the major silver site is subject to large-amplitude thermal vibration, although about a position still close to the position that optimises the silver coordination. There is, however, evidence for limited occupation by silver of the ABR site suggesting that the activation energy for conduction will be small. In the low-angle region of the observed diffraction profile (figure 2), the superlattice reflections (Boilot *et al* 1979a, b, 1980, Newsam and Tofield 1981b) are still present, but of reduced intensity compared with the data at 4.2 K. This change manifests the breakdown of long-range ordering within the conduction planes. The structural parameters indicate, however, that the silver atoms do not yet adopt the quasi-liquid (two-dimensional) distribution that is apparent at 500 °C (see below).

The c-axis lattice constant, $c = 22.5293(2)$ Å (table 1), is still increased relative to the non-stoichiometric parent, $c = 22.488$ Å (Roth 1972), reflecting both the absence of interstitial defects and the reduced cation density in the mirror planes (which therefore provides less cohesion between the similarly charged oxide ion layers that bound these planes). The parameters of the spinel block atoms (table 2) are in close agreement with those of Colomban and co-workers (Colomban 1979, Boilot *et al* 1980), although the details of the mirror plane distributions differ somewhat. We have found no evidence for occupation of sites close to the BR position, but there is an indication of some ABR occupation. Colomban and co-workers (Colomban 1979, Boilot *et al* 1980) also report a significant population of interstitial aluminium atoms. These small, but important

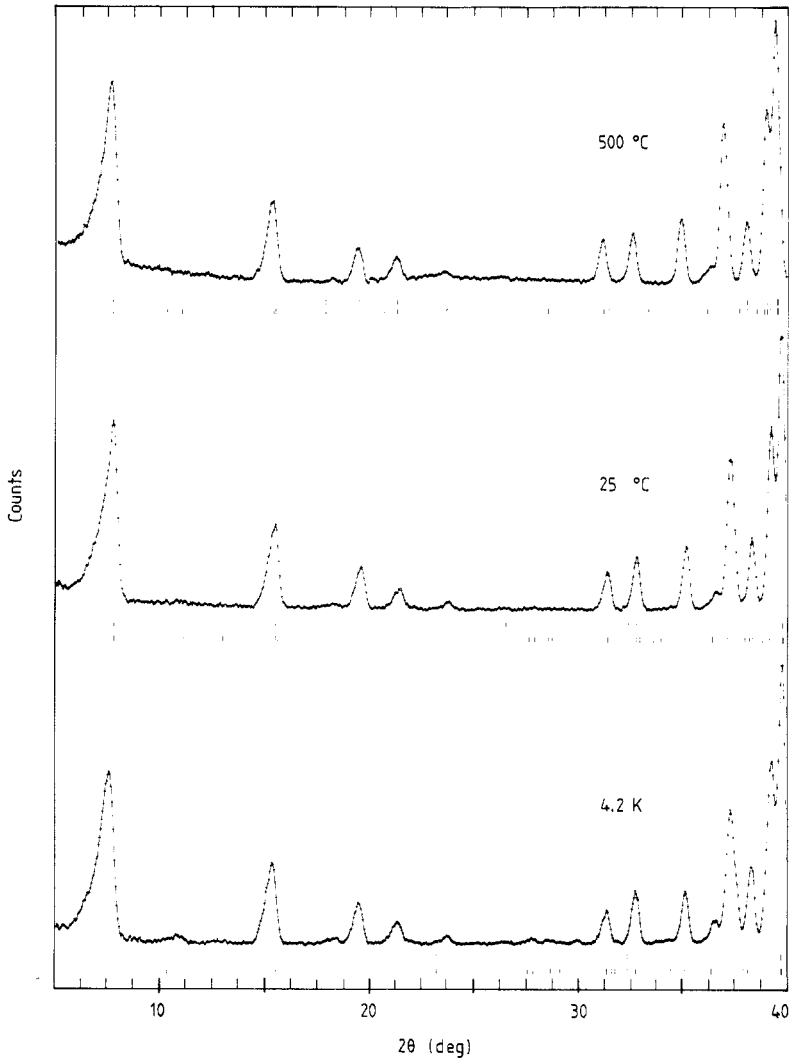

Figure 2. The low-angle regions of the observed powder neutron diffraction profiles for $AgAl_{11}O_{17}$ at 4.2 K (bottom), 25 °C (centre), and 500 °C (top). The upper faint vertical bars indicate in each case the positions of reflections allowed on the basis of the normal beta alumina unit cell (as appear also in figures 1 and 4). The lower sets of bars indicate the reflection positions for the $a\sqrt{3} \times a\sqrt{3} \times c$ supercell (Boilot *et al* 1980, Newsam and Tofield 1981b).

differences probably arise from the different preparation routes used. The near-stoichiometric silver beta alumina of Colomban and co-workers was prepared via the thermal decomposition of non-stoichiometric ammonium beta lumina, which, in structural terms, evolves through a rather complicated series of stages (Newsam *et al* 1983).

At 500 °C, the refinement results indicate that the silver atom distribution is highly diffuse, indicative of the quasi-liquid distribution that had been deduced for the stoichiometric material in x-ray diffuse scattering studies (Boilot *et al*, 1979a, b, 1980). The weak superlattice reflections have now disappeared from the low-angle region of the diffraction profile (figure 2). It is interesting to compare this model with that derived by

Table 3. Bond distances (Å) with estimated standard deviations in parentheses calculated from the final coordinates for $AgAl_{11}O_{17}$ and $Ag_{1-x}Al_{11}O_{17+x/2}$.

	Number of bonds	Stoichiometric					Non-stoichiometric	
		4.2 K†	25 °C	300 °C	500 °C	550 °C‡	25 °C§	25 °C‖
Octahedra								
Al(1)–O(1)	2	2.021(2)	2.023(3)	2.024(8)	2.043(3)	2.040	2.026(4)	2.017
–O(2)	2	1.830(2)	1.832(3)	1.847(8)	1.828(3)	1.843	1.832(4)	1.839
–O(3)	1	1.992(3)	1.990(3)	1.988(10)	1.990(4)	1.986	1.981(5)	1.973
–O(4)	1	1.793(1)	1.799(3)	1.791(10)	1.816(3)	1.822	1.811(5)	1.821
Average		1.914(1)	1.917(1)	1.920(4)	1.925(1)	1.929	1.918(2)	1.918
Al(4)–O(1)	6	1.897(2)	1.891(2)	1.879(5)	1.907(2)	1.898	1.885(3)	1.893
Tetrahedra								
Al(2)–O(1)	3	1.791(2)	1.796(2)	1.816(7)	1.798(2)	1.806	1.809(4)	1.806
–O(3)¶	1	1.799(6)	1.814(5)	1.804(18)	1.821(6)	1.828	1.799(9)	1.800
Average		1.793(2)	1.800(2)	1.813(5)	1.804(2)	1.811	1.807(3)	1.804
Al(3)–O(2)	3	1.769(4)	1.764(3)	1.797(7)	1.774(3)	1.756	1.772(4)	1.762
–O(5)	1	1.716(7)	1.704(5)	1.635(12)	1.704(8)	1.716	1.686(9)	1.675
Average		1.756(2)	1.749(1)	1.757(4)	1.757(2)	1.746	1.750(3)	1.740
Silver contacts								
Ag(1)–O(2)	4	2.727(3)	2.724(5)	2.709(9)	2.727(12)	—	2.70(1)	2.720
–O(5)	2	2.595(9)	2.70(1)	2.73(3)	2.76(5)	—	2.77(3)	—
Ag(2)–O(4)	2	—	2.431(2)	2.44(1)	2.436(5)	—	2.421(3)	2.424
–O(5)	3	—	2.96(2)	2.89(2)	3.03(3)	—	2.91(3)	3.117
Ag(3)–O(4)	2	—	—	—	—	—	2.51(5)	—
–O(5)	2	—	—	—	—	—	2.64(11)	—

† Newsam and Tofield (1981b).
‡ Tofield *et al* (1979).
§ Neutron diffraction study of partially reduced large single crystal (Newsam 1980).
‖ Roth (1972).
¶ Symmetry operator 13 has been applied (Hahn 1983).

Reidinger for the non-stoichiometric sodium beta alumina at 500 °C (Reidinger 1979). In that material, the degree of thermal motion increases and the distribution between BR, MO and ABR sites is altered as the temperature is raised from 80 K to 500 °C, but the sodium scattering density remains well defined. The anisotropic temperature factors do not become excessively large, even at 500 °C. The x-ray diffuse data on non-stoichiometric sodium beta alumina (Boilot *et al* 1978) do not display the quasi-liquid scattering that is found for both non-stoichiometric (Boilot *et al* 1976) and near-stoichiometric silver beta aluminas (Boilot *et al* 1979b) and because of this difference, the effect of the absence of interstitial mirror plane oxygen ions (and off-plane aluminium interstitials) on the cation distributions in the stoichiometric materials at elevated temperatures cannot be gauged directly. To complete the comparison between the sodium and silver beta alumina systems, it would be interesting to examine, as a function of temperature, the structure of the stoichiometic sodium compound, $NaAl_{11}O_{17}$.

Examination of the atomic coordinates (table 2, and Newsam and Tofield 1981a) and bond lengths and angles (tables 3 and 4) as a function of temperature demonstrates that the spinel block atoms are little affected by the order–disorder transition that occurs within the mirror planes. This is consistent with the description of the superlattice

Table 4. Bond angles (deg) with estimated standard deviations in parenthesis calculated from the final coordinates for $AgAl_{11}O_{17}$ and $Ag_{1-x}Al_{11}O_{17+x/2}$.

		Stoichiometric				Non-stoichiometric	
	4.2 K†	25 °C	300 °C	500 °C	550 °C‡	25 °C§	25 °C‖
Octahedra¶							
O(1)–Al(1)–O(1)^2	81.6(1)	81.2(2)	80.6(4)	81.1(1)	80.0	80.6(2)	—
–O(2)	90.2(1)	90.2(1)	91.0(3)	90.0(1)	90.1	90.8(1)	90.70
–O(3)	88.4(1)	88.5(1)	88.8(4)	88.4(1)	88.7	88.7(2)	89.19
–O(4)	84.2(1)	84.4(1)	84.4(5)	83.9(2)	83.9	83.9(2)	84.04
O(2)–Al(1)–O(2)^2	97.2(2)	97.8(2)	96.7(5)	98.2(2)	98.5	97.3(2)	—
–O(3)	85.4(1)	85.3(1)	85.0(4)	85.6(1)	86.0	85.9(2)	86.09
–O(4)	101.0(1)	100.8(1)	100.8(5)	100.9(2)	100.2	100.4(2)	—
O(1)–Al(4)–O(1)^2	88.3(1)	88.2(1)	88.3(2)	88.4(2)	88.3	88.0(1)	92.06
Tetrahedra							
O(1)–Al(2)–O(1)^2	110.6(1)	110.9(1)	110.5(4)	110.7(2)	111.1	110.6(2)	110.37
–O(3)^{13}	108.3(1)	108.0(2)	108.4(4)	108.2(1)	107.8	108.3(2)	108.56
O(2)–Al(3)–O(2)^2	106.9(2)	106.8(2)	104.6(4)	107.0(2)	107.4	106.7(2)	107.55
–O(5)^2	105.7(3)	107.4(5)	107.6(8)	108.0(9)	—	106.5(5)	111.33
Silver Contacts							
O(5)–Ag(1)–O(5)^2	147.5(4)	144.4(8)	133(1)	143(2)	—	132.0(2)	—
–O(2)^{17}	62.9(1)	62.1(2)	61.2(4)	61.7(5)	—	60.8(3)	—

† Newsam and Tofield (1981b).
‡ Tofield *et al* (1979).
§ Neutron diffraction study of partially reduced large single crystal (Newsam 1980).
‖ Roth (1972).
¶ Superscript numerals refer to the number of the symmetry operator that has been applied (Hahn 1983).

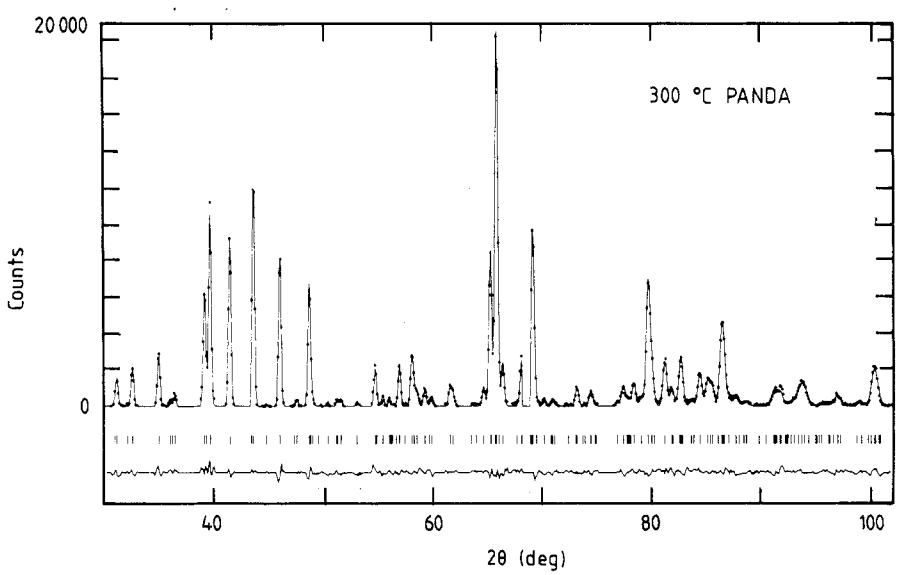

Figure 3. The final observed, calculated and difference powder neutron diffraction profiles for stoichiometric silver beta alumina at 300 °C (legend as for figure 1).

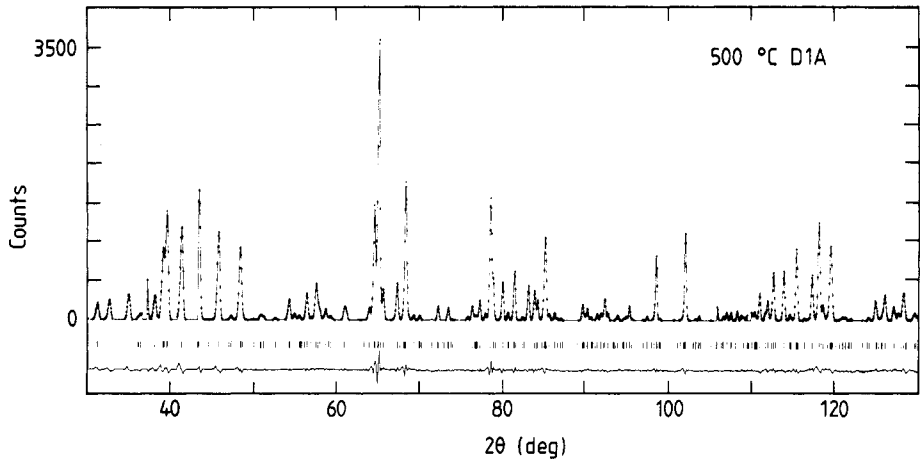

Figure 4. The final observed, calculated and difference powder neutron diffraction profiles for stoichiometric silver beta alumina at 500 °C (legend as for figure 1).

observed at 4.2 K as deriving solely from the silver location and the cooperative displacement of O5. As the silver becomes more delocalised, the effective strength of the Ag–O5 interaction diminishes and the extent of the displacement of O5 away from the 2c site decreases. This is manifested by an increase in the O5 x-parameter from 4.2 K to 25 °C to 500 °C. At these three temperatures, the Al3–O5 bond length is increased relative to the non-stoichiometric material; the bond length observed in a partially reduced, large single-crystal specimen (Newsam 1980) is intermediate between the two. This local change in the Al3–O5 bond length is presumably coupled to the changes in the c-axis constant that accompany modifications of the stoichiometry.

Acknowledgments

We thank A W Hewat for assistance with the neutron diffraction measurements, W A England for donation of the sample, and the Science Research Council for the provision of neutron scattering facilities. JMN also thanks AERE Harwell for financial support under the terms of research contract H4B2952EMR.

References

Bates J B and Farrington G C eds 1981 *Fast Ionic Transport in Solids; Solid State Ionics* **5**

Boilot J P, Colomban P, Collin G and Comes R 1979a *Fast Ion Transport in Solids* ed. P Vashishta, J N Mundy and G K Shenoy (New York: Elsevier–North-Holland) pp 243–7

—— 1980 *J. Phys. Chem. Solids* **41** 47–54

Boilot J P, Colomban P, Collongues R, Collin G and Comes R 1979b *Phys. Rev. Lett.* **42** 785–7

Boilot J P, Colomban P, Thery J, Collin G and Comes R 1978 *J. Physique Coll.* **39** C7 145–50

Boilot J P, Thery J, Collongues R, Comes R and Guinier A 1976 *Acta Crystalogr.* A **32** 250–5

Boyce J B, De Jonghe L C and Huggins R A (eds) 1985 *Solid State Ionics—85; Solid State Ion.* **18, 19**

Collongues R, Gourier D, Kahn A, Boilot J P, Colomban P and Wicker A 1984 *J. Phys. Chem. Solids* **45** 981–1013

Colomban P 1979 *DSc These* Universite Pierre et Marie Curie, Paris

England W A, Jacobson A J and Tofield B C 1982 *Solid State Ion.* **61** 21–7

Hahn T (ed) 1983 *International Tables for Crystallography* vol A (Dordrecht: Riedel)

Hewat A W and Bailey I 1976 *Nucl. Instrum. Methods* **137** 463–71
Howard C J 1982 *J. Appl. Crystallogr.* **15** 615–20
Kleitz M, Sapoval B and Chabre Y (ed.) 1983 *Solid State Ionics—83; Solid State Ion.* **9, 10**
Kummer J T 1972 *Prog. Solid State Chem.* **7** 141
Newsam J M 1980 *PhD Thesis* Oxford University
Newsam J M, Cheetham A K and Tofield B C 1983 *Solid State Ion.* **8** 133–9
—— 1985 *J. Solid State Chem.* **60** 214–29
Newsam J M and Tofield B C 1981a *Solid State Ion.* **5** 59–64
—— 1981b *J. Phys. C: Solid State Phys.* **14** 1545–54
Prince E 1983 *J. Appl. Crystallogr.* **16** 508–11
Reidinger F 1979 *DPhil Thesis* New York State University
Rietveld H M 1969 *J. Appl. Crystallogr.* **2** 65–71
Roth W L 1972 *J. Solid State Chem.* **4** 60–75
—— 1975 *Crystal Structure and Chemical Bonding in Inorganic Chemistry* ed. C J Rooymans and A Rabenau pp 85–102
Tofield B C, England W A, Jacobson A J, Clarke P J and Thomas M W 1979 *J. Solid State Chem.* **30** 1–22
van Laar B and Yelon W B 1984 *J. Appl. Crystallogr.* **17** 47–54